A Multi-Temporal Assessment of Urban Growth Patterns in Argungu, Kebbi State, Nigeria Using Geospatial Techniques

Ebenezer Ayobami Akomolafe *, Abdulazeez Onotu Aliyu, Swafiyudeen Bawa, Mefe Moses,
Saadu Ya'u, and Rahama Muhammad Isah

Department of Geomatics, Ahmadu Bello University, Zaria, Nigeria – eaakomolafe@abu.edu.ng, aoaliyu@abu.edu.ng, bswafiyudeen@abu.edu.ng, mmoses@abu.edu.ng, saadyaukangiwa6@gmail.com, ramcycool131@gmail.com

Keywords: Geospatial, Multi-temporal, Urban sprawl, Shannon's Entropy, Land Use Land Cover (LULC), Argungu.

Abstract

This study employs geospatial analysis using Shannon's Entropy to quantify urban sprawl over four epochs (2009, 2013, 2018, and 2023) in Argungu, Kebbi state, Nigeria, which is currently facing rapid urbanization. By analyzing multi-temporal Landsat imagery, the research identifies land use and land cover (LULC) changes and assesses the uncontrolled expansion of urban areas, contributing to habitat fragmentation and infrastructure pressure. The imagery was classified into five LULC classes: built-up, bare land, rock, water body, and vegetation through a supervised classification approach. Results revealed a significant increase in built-up areas, from 2,192.65 hectares in 2009 to 4,277.22 hectares in 2023, with built-up sprawl primarily spreading in the North-East and North directions. Water bodies initially increased due to flooding but declined by 2023. Entropy values increased from 0.724 in 2009 to 0.819 in 2023, indicating a shift from compact urban forms to fragmented landscapes. The study underscores the value of remote sensing and Shannon's Entropy in monitoring urban growth dynamics, providing essential perceptions for sustainable urban planning and management of both natural and man-made resources in Argungu.

1. Introduction

Across the globe, cities are expanding at an unprecedented rate, a phenomenon fuelled by urbanization and economic development that is often referred to as urban sprawl (Steurer and Bayr, 2020). Sadigov (2022) noted that this rapid growth presents a double-edged sword, offering opportunities and prosperity while also posing significant challenges to social and environmental well-being. Urbanization itself, which is the increasing concentration of people in urban areas leading to the development of towns and cities, is influenced by a complex interplay of social, political, and geographical factors, which cause its manifestations to vary from one location to another (Isma'il et al., 2015). Urbanization, which is a prominent global trend that gained momentum since the twentieth century, stands out as a main driver in reshaping landscape structure and functions. Conversely, Land use land cover (LULC) change constitutes a very important variable influencing resource planning, control measures, and contamination of vital resources of the earth, such as soil and water (Behera et al., 2025).

For the past thirty years, urban sprawl has been a significant trend in developing nations, attracting attention from various academic fields (Ankrah et al., 2024; Zhu et al., 2024). This sprawl can be quantitatively defined by the amount of built-up area and its degree of dispersion across the landscape (Jaeger et al. 2010). Describing and understanding these dynamic patterns of urban growth is imperative, as urbanization remains a major driver of global environmental transformation. Consequently, the process poses significant challenges to sustainable development and effective urban planning.

Nigeria exemplifies this trend as one of the most urbanized countries in Africa, with an annual urbanization rate of 3.5% (Musa and Abubakar, 2024). Within this context, Argungu town in Kebbi State, which originated as a nucleus settlement, has undergone tremendous urban expansion. This rapid and often unplanned growth threatens agricultural lands, natural resources, and socio-economic stability (Lawal and Gulma, 2024).

Presently, the urban growth rate in Argungu is accelerating, driven by factors such as the Argungu International Fishing and Cultural Festival, agricultural activities, and emerging industries like the Wacot Rice Plc. production plant. This expansion has led to increased environmental problems, including congestion, pollution, and sprawling along the city's edges. Shikary and Rudra (2021) noted that LULC change plays an essential role to determine the potential use of natural resources but however, the insatiable demand for land use changes by population pressure rises detrimental effect on natural and agricultural lands.

Despite these evident impacts, there is a critical lack of comprehensive monitoring and prediction systems tailored to Argungu's unique characteristics. The key problems associated with sprawl in the town include a lack of spatial planning, environmental degradation, infrastructure deficiencies, socio-economic disparities, and future uncertainty (Lawal and Gulma, 2024). As a result, the assessment of the spatial pattern, drivers, rate of growth, and management of urban sprawl has remained unresolved over the years.

Fortunately, advancements in remote sensing and GIS techniques now provide viable options for urban sprawl to be effectively mapped and monitored (Bielecka, 2020; Wiatkowska et al., 2021). Furthermore, predicting future scenarios of urban expansion helps us anticipate potential impacts and proactively guide sustainable development strategies. Cellular automata (CA) and machine learning (ML) are widely used modeling approaches (Taloor, et al., 2020, Nyamekye et al., 2021; Sajan et al., 2022;). CA models simulate urban expansion based on defined transition rules and interactions between neighboring areas, while ML algorithms learn complex relationships from

historical data to forecast future patterns (Sakizadeh et al., 2024). Choosing the right model depends on data availability, desired level of complexity, and specific research objectives.

In view of the aforementioned problems, this study is aimed at spatiotemporally investigating the urban growth pattern in the study area and projecting for near-future changes. Monitoring urban growth patterns and predicting future trends in Argungu is essential for fostering sustainable development, preserving natural resources, enhancing resilience, and promoting inclusive growth within the region and beyond.

2. Study Area

The study area is Argungu Local Government Area of Kebbi state, Nigeria. Geographically, it is located between Latitudes 12o 28' 52'' and 12o 51' 46" North of the Equator and between Longitudes 4o 05' 25'' and 4o 50' 18" East of the Central Meridian, covering a total land mass of approximately 120,280 Hectares. Characterized by a tropical wet and dry climate, the region experiences a yearly average temperature of 26°C, which can escalate to 40°C during the peak hot season from March to July, with an average annual rainfall of about 800mm. Argungu LGA is home to 342,100 people, according to population projections for 2022 (Lawal and Gulma, 2024). The landscape predominantly consists of dry, arid plains interspersed with scattered hills and elevated landforms, and is hydrologically defined by numerous rivers, streams, ponds, and pools, most notably the River Rima and the Gulbin Kabi. The local economy is primarily agrarian, with a focus on rice cultivation and fishing. A significant cultural and economic driver is the Argungu International Fishing and Cultural Festival, a major tourist attraction alongside the Kanta Museum. A map defining the study area is shown in Figure 1.

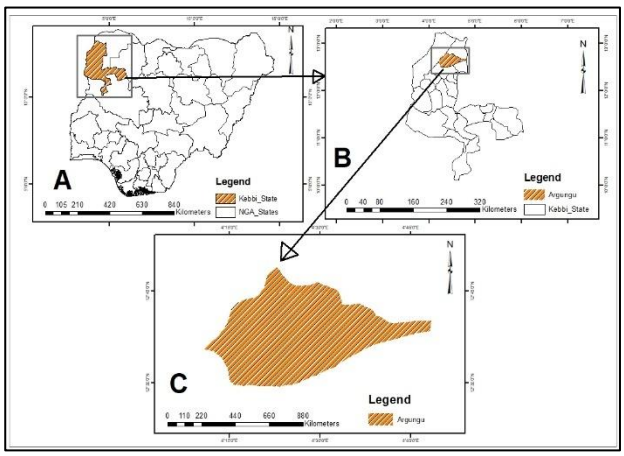

Figure 1. The location of the study area.

3. Methodology

3.1 General Workflow

The methodological flow for spatiotemporal assessment of growth pattern in the area under study followed a structured sequence, as seen in Figure 2.

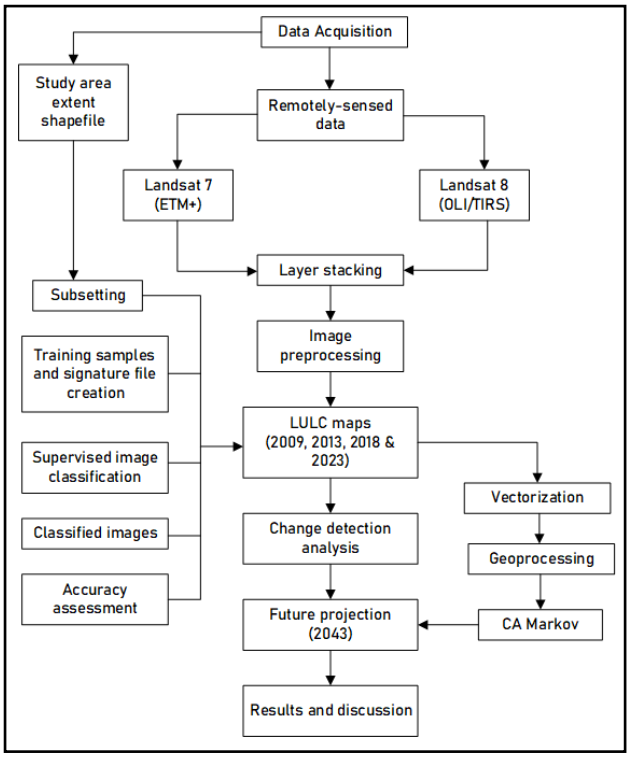

Figure 2. Methodological workflow diagram adopted.

It starts begins with the acquisition and pre-processing of multi-temporal satellite imagery, including radiometric correction. Supervised classification was then applied to the processed imageries followed by change detection analysis. The classified maps were assessed for accuracy using high-resolution reference data and finally analyzed and visualized within a GIS environment to quantify and interpret the spatial patterns of observed land cover or land use changes.

3.2 Data acquisition and correction

Cloud-free Landsat ETM+ (EROS, 2020a) and Landsat OLI/TIRS (EROS, 2020b) raster data of the study area for the years 2009, 2013, 2018 and 2023 were obtained from the United States Geological Survey (USGS) website. Table 1 provides a summary of the dataset used.

Satellite/sensor	Path/Row	Acquisition date	Spatial resolution
Landsat 7 (ETM+)	191/051	29-11-2009	30m
Landsat 8 (OLI/TIRS)	191/051	29-09-2013	30m
	191/051	14-11-2018	
	191/051	27-10-2023	

Table 1. Characteristics of dataset used

The Landsat data were subjected to radiometric correction to reduce the visual complexity of the images and also to improve the visual quality and recognition of features for the purpose of easy image interpretation. All raster and vector data used in this study were reprojected into the same coordinate system (UTM Zone 32N on WGS84 ellipsoid). This is to ensure consistency and to aid subsequent analyses. A subset of each epoch of the layer-stacked Landsat images was generated to align with the administrative boundary of the study area.

3.3 Image classification

The overall objective of image classification is to automatically categorize all pixels in an image into land cover classes or themes. In this study, a supervised classification approach was employed using a maximum likelihood algorithm. Supervised image classification is a technique that involves training a model using labelled data to classify pixels in images into predefined categories, such as LULC type. The images were classified into five (5) Land use and Land cover (LULC) classes namely; Built-up, bare land, rock, water body, and vegetation. The major procedures adopted in the classification of the images, per epoch include: selection of training samples, creation of signature files, classification and accuracy assessment.

3.4 Change detection

Area differential analysis was adopted as the change detection technique in this study after image classification of each epoch i.e. 2009, 2013, 2018, and 2023, change detection was carried out. This was done to highlight the trend and changes in the different LULC classes within the period under assessment. Here, the transition from one class to another was also computed in a GIS environment.

3.5 Shannon's entropy

Shannon's entropy was used as a method to determine the urban growth pattern of Argungu. The changes in entropy value can be used to identify whether land development is towards a dispersed (sprawl) or compact pattern. The entropy is calculated using the formula:

$$H_n = -\sum_{i=1}^{n} P_i \log_e(P_i), \quad (1)$$

where
P_i = probability of a phenomenon (variable) occurring in the i^{th} zone ($P_i = \frac{x_i}{\sum x_i}$)
x_i = the observed value of the variable in the i^{th} zone,
n = the total number of zones/grids

The range of Shannon's entropy value varies from 0 to $\log_e(n)$. Values closer to zero means that built up features are extremely compact in distribution, while values closer to $\log_e(n)$, and indicates the scattered distribution of built-up areas. Higher entropy values highlight sprawl occurrence. The threshold value to categorize sprawl and non-sprawl is taken as the mid-way mark of $\log_e(n)$. If a city crosses its threshold entropy value, it is said to be a sprawling city.

Shannon's entropy model was calculated using buffer zones and direction-wise methods. In this study, direction-wise method was applied for monitoring the urban growth in different directions. The ring buffers around the urban boundary were divided into 8 sectors (directions), from the centre of the urban area to explore the sprawling in various directions.

3.6 Future projection of urban growth

Markov chain model was used in QGIS to obtain the future predicted change in LULC of Argungu L.G.A. of Kebbi state, Nigeria. This projection was accomplished by developing a transition probability matrix of the change in land use from time one (t_1) to time two (t_2). Using existing geographical variables like road network and DEM, the Markov model was used to predict the spatial trend and patterns of land use in 2043. To model a process of land use change by Markov chain, the land cover distribution at (t_2) is calculated from the initial land use and land cover distribution at (t_1) by means of transition matrix as follows:

$$vt_2 = (M \times vt_1), \quad (2)$$

where
vt_1 = the input LULC proportion column vector
vt_2 = the output LULC proportion column vector
M = an m x m transition matrix for the time interval $\Delta t = t_2 - t_1$.

4. Results and Discussion

4.1 Spatiotemporal Pattern of LULC

The results of the classified images of 2009, 2013, 2018, and 2023 of the study area are displayed in Figure 3 (a), (b), (c), and (d) respectively. The figure highlights the spatial pattern and changes in LULC over a 20-year study period. Table 2 shows a summary of the metrics of the spatial distribution of classes in the LULC maps.

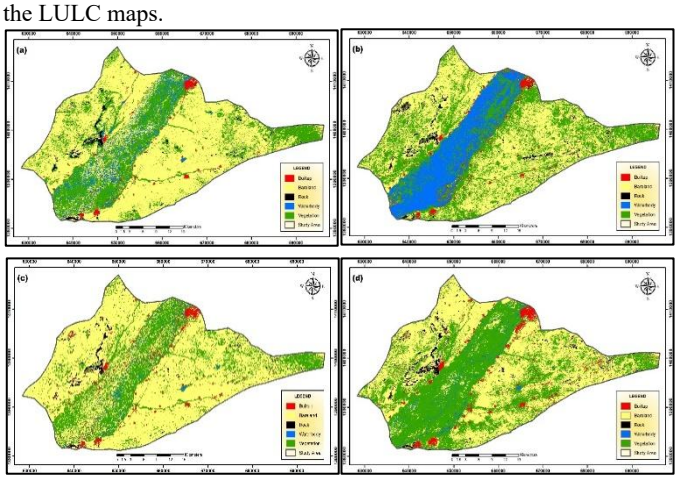

Figure 3. Spatial distribution of LULC in (a) 2009, (b) 2013, (c) 2018 and (d) 2023.

LULC class	Area covered (in Hectares)			
	2009	2013	2018	2023
Builtup	2192.65	2856.61	3988.00	4277.22
Bareland	76782.66	52112.25	82901.00	58661.08
Rock	2205.92	2558.16	1657.82	2928.27
Waterbody	4736.67	20776.70	1519.12	1809.07
Vegetation	34364.66	41978.85	30216.62	52606.92
TOTAL	120282.56	120282.56	120282.56	120282.56

Table 2. Metrics of spatial pattern of LULC distribution.

The Built-up area showed a consistent, sustained growth trend across all epochs, nearly doubling its coverage from 2,192.65 Ha (1.82%) in 2009 to 4,277.22 Ha (3.56%) in 2023. This increase is attributed to population growth, economic activities, and improved accessibility which encourages residential and commercial development. Bare surface covered 76,782.66 Ha (63.84%) of the land mass in 2009, experience declined to 52,112.25 Ha (43.32%), in 2013 due to the flooding that occurred within the period. It however increased to 82,901.00 Ha (68.92%) in 2018 after the flood. Figure 4 shows graphically, the percentage distribution of each LULC class between 2009 and 2023.

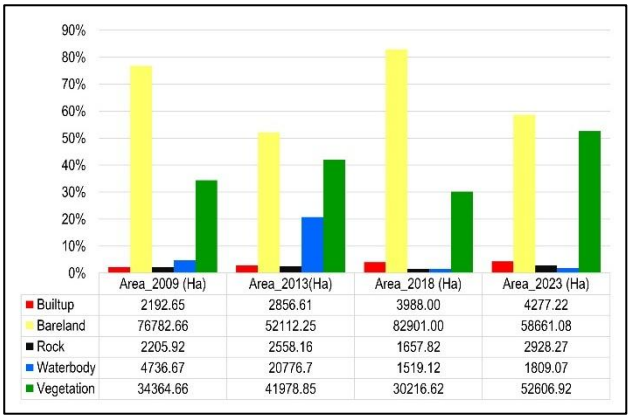

	Area_2009 (Ha)	Area_2013(Ha)	Area_2018 (Ha)	Area_2023 (Ha)
Builtup	2192.65	2856.61	3988.00	4277.22
Bareland	76782.66	52112.25	82901.00	58661.08
Rock	2205.92	2558.16	1657.82	2928.27
Waterbody	4736.67	20776.7	1519.12	1809.07
Vegetation	34364.66	41978.85	30216.62	52606.92

Figure 4. Spatiotemporal pattern of classified land cover classes

Water body increased from 4,736.67 Ha (3.94%) in 2009, to 20,776.70 Ha (17.27%), in 2013 due to the flood along the Argungu river area. However, in 2018, it occupied 1,519.12 Ha (1.26%), falling below the initial 2009 level after the floodwaters receded. Vegetation exhibited a dynamic pattern strongly linked to the bare land class and the Argungu river. It showed a significant net increase from 34,364.66 Ha in 2009 to 52,606.92 Ha in 2023, suggesting successful re-vegetation or replenishment after the flooding. Most changes in the Vegetation occurred randomly around the Argungu river, as seen in Figure 3.

4.1.1 Accuracy assessment: The accuracy assessment of LULC classification from 2009 to 2023 was carried out in a GIS environment. It shows clear trends of improvement and challenges in classification across various land use and cover types. Table 3 shows the results of the accuracy assessment.

Classes	2009		2013		2018		2023	
	PA (%)	UA (%)	PA (%)	UA (%)	PA (%)	UA (%)	PA (%)	UA (%)
Built-up	60	75	70	70	90	82	88	70
Bare land	91	94	87	91	95	91	78	96
Rock	0	0	69	90	67	100	88	70
Water body	88	88	100	69	100	80	88	70
Vegetation	87	77	85	88	100	95	91	75
Kappa statistics	0.7670		0.7900		0.8494		0.7373	
Overall Accuracy	65.2%		82.2%		90.4%		86.6%	

PA= Producer Accuracy, UA= User Accuracy

Table 3. Accuracy assessment of LULC classification.

The Kappa statistics indicate consistently substantial to strong agreement across all epochs (between 0.7373 and 0.8494), confirming the reliability of the LULC classifications. The estimated overall accuracy (OA) of the land use/land cover (LULC) classifications demonstrates a clear temporal improvement, indicating increasing classification reliability over time. The OA increased markedly from 65.2% in 2009 to 82.2% in 2013, suggesting substantial enhancement in classification performance. The highest estimated accuracy was achieved in 2018, with an OA of 90.4%, reflecting excellent thematic consistency and strong class separability. This peak performance may be associated with improved sensor characteristics, optimal image acquisition conditions, and increased robustness of classification algorithms. In 2023, the estimated OA declined slightly to 86.6%, although it remained within a high accuracy range. The slight decline in OA in 2023 is likely due to increased landscape heterogeneity and mixed land-use patterns. Overall, the estimated OA values indicate that the LULC classifications are sufficiently accurate to support multi-temporal change detection and trend analysis.

4.2 Change detection analysis

As seen in Table 4, the gain and loss analysis between 2009 and 2023 reveals a dynamic landscape driven by both urbanization and acute environmental events. Built-up areas showed a steady, near-doubling expansion (+95.04%), with the most rapid development occurring between 2013 and 2018, reflecting sustained urban growth pressures. In contrast, Waterbody class spiked dramatically between 2009 and 2013 (+338.58%) due to flooding, followed by a drastic subsequent decline (−92.69%), suggesting post-flood water depletion.

The bare land class initially decreased due to the flood but rose again between 2013 and 2018. Vegetation class, which achieved a significant overall net gain (+53.08%) due to a massive surge in the most recent period (2018–2023), indicates successful environmental restoration efforts following a temporary loss after the flooding.

LULC class	2009 - 2023		2013 - 2018		2018 - 2023		2009-2023	
	Δ Area coverage (Ha)	Δ Area coverage (%)	Δ Area coverage (Ha)	Δ Area coverage (%)	Δ Area coverage (Ha)	Δ Area coverage (%)	Δ Area coverage (Ha)	Δ Area coverage (%)
Builtup	663.96	30.28	1131.39	39.61	289.22	7.25	2084.57	95.07
Bareland	-24670.41	-32.13	30788.75	59.08	-24239.92	-29.24	-18121.58	-23.60
Rock	352.24	15.97	-900.34	-35.19	1270.45	76.64	722.35	32.75
Waterbody	16040.03	338.64	-19257.58	-92.69	289.95	19.08	-2927.60	-61.81
Vegetation	7614.19	22.16	-11762.23	-28.02	22390.30	74.12	18242.26	53.08

Table 4. Area and percentage gain and loss between 2009 and 2023.

4.3 Shannon's Entropy

To the intensity and level of changes of Argungu, relative entropy values was calculated for each year under study. The Shannon's entropy analysis focused mainly on the urban centre (Argungu town) for the analysis of the urban growth pattern in the area. The centre of the urban boundary was place within 8 cardinal directions (N: North, NE: Northeast, E: East, SE: Southeast, S: South, SW: Southwest, W: West and NW: Northwest), to explore the sprawling in various directions. This approach was also used to generate the size of the built-up area along the direction in each buffer zone. Figure 5 shows the buffer zones and cardinal directions used for the entropy computation and the spatial pattern of spread of the built-up area in each direction. The obtained quantitative values are summarized in Table 5.

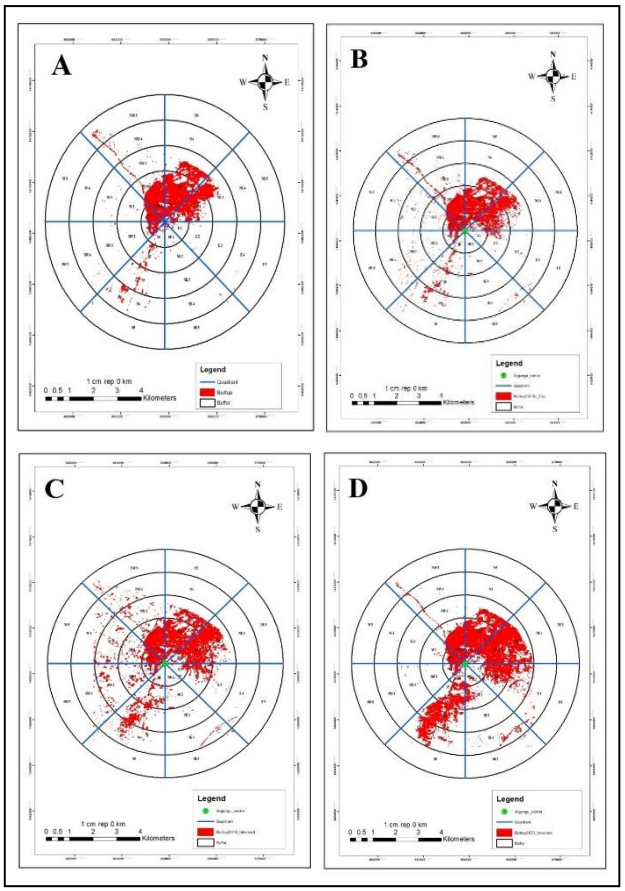

Figure 5. Division of buffer zones for measuring built-up size in (a) 2009, (b) 2013, (c) 2018 and (d) 2023.

Quadrant	Built-up area (Ha)				Total area (Ha)
	2009	2013	2018	2023	
N	171.96	159.21	160.68	178.15	670.00
NE	116.64	143.13	188.59	240.03	688.39
E	4.66	14.40	46.21	121.67	186.94
SE	3.27	5.08	11.81	41.35	61.49
S	36.42	41.94	93.70	224.84	396.90
SW	18.29	18.57	52.31	15.21	104.37
W	32.84	38.62	71.05	34.52	177.02
NW	96.19	113.76	120.33	104.09	434.36

Table 5. The size of urban built-up area in different directions from 2009 to 2023

The built-up area shows a consistent growth pattern over the entire 2009–2023 period, expanding outwards from the center toward the periphery across all buffer zones. Urban sprawl has primarily expanded toward the Northeast (NE), North (N) and South (S) directions, indicating these are the areas of most robust growth. The Southeast (SE) and Southwest (SW) quadrants have experienced more fluctuation in growth, suggesting less consistent development. The variations in growth across different directions highlight the dynamic nature of urban growth, which is influenced by a combination of market demands, infrastructure developments, and land-use policies that have shaped the trajectory of growth in the urban landscape. Table 6 shows the overall relative entropy per epoch in the study period. This is

important so as to determine the pattern of growth of the urban area over the years in Argungu.

Epoch	Shannon's entropy	Remarks
2009	0.7244	This result shows a scattered pattern of sprawl.
2013	0.7456	This result shows a scattered pattern of sprawl
2018	0.8178	This result shows a scattered pattern of sprawl
2023	0.8190	This result shows a scattered pattern of sprawl

Table 6. Shannon's entropy values in the years 2009, 2013, 2018 and 2023.

In Argungu, the Shannon's entropy values in the years 2009, 2013, 2018 and 2023 reflect a trend toward increasing sprawl. 2009 has an entropy value of 0.7244. The value indicates a relatively lower level of mixed land use, suggesting Argungu was more homogeneously developed at this time. In 2013, with a value of 0.7456, this slight increase suggests an early sign of sprawl and a marginal diversification in land use, with more varied land uses beginning to emerge. 2018's value (0.8178) shows a marked increase in diversity, implying that development became more scattered and varied. This rise reflects substantial residential expansion, commercial growth, and possibly a shift toward more informal land uses. The minimal increase in entropy value from 0.8178 in 2018 to 0.8190 in 2023 suggests that while sprawl continued, the rate of change has stabilized somewhat. The land use remains diverse, but the rapid changes observed in earlier periods appear to be slowing down. The overall entropy trend confirms an increasing trend towards sprawl in Argungu, which the analysis identifies as consistent with low-density, leapfrog development.

4.4 Projection of Future LULC Change

Markov chain analysis was used to predict the changes in LULC over a 20-year period between 2023 and 2043. Result in shown as a map in Figure 6. Table 7 shows a summary of the changes between 2023 and 2043 quantitatively.

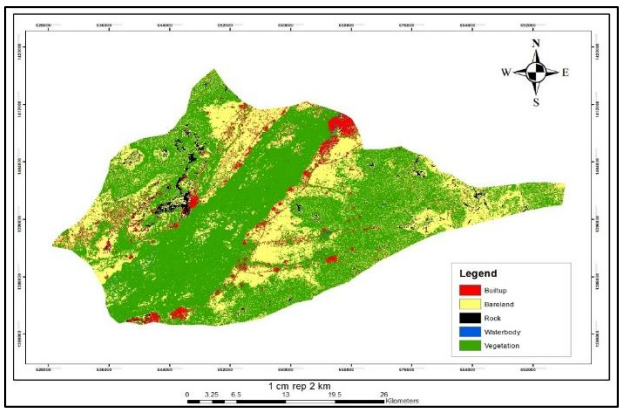

Figure 6. Markov model-projected LULC of Argungu L.G.A. to 2043.

The analysis of the past changes in land use land cover spatial distribution gives rise to the assessment of the extent to which urban sprawl might change in the future.

LULC class	2023		2043		Δ Area (2023-2043) (Ha)
	Area covered (Ha)	(%)	Area covered (Ha)	(%)	
Builtup	4277.22	3.56	6495.93	5.40	2218.71
Bareland	58661.01	48.77	37671.39	31.32	-20989.70
Rock	2928.24	2.43	2516.8	2.09	-411.47
Waterbody	1809.07	1.50	670.95	0.56	-1138.12
Vegetation	52606.91	43.74	72927.49	60.63	20320.57
TOTAL	120282.56	100	120282.56	100	

Table 7. LULC class changes between 2023 and 2043.

It is projected that in 2043, about (6495.93 Ha) of the total land will be Builtup, consuming 5.40% of the total land mass in Argungu. This is a clear indication of urban growth by that year, due to high demand for land. Consequently, this will affect the coverage of bare land, rock, and water body. It is predicted that bare land will have diminished by 20989.70 Ha by 2043. This is attributed to the increase in built-up and the increasing need of land for urban development. However, vegetation cover is projected to increase from 52606.91 Ha (43.74%) in 2023 to 72927.49 Ha (60.63%) in 2043. The increase in urban area will result in an increased demand for food. The increase in vegetative cover is attributed to increased cultivation of food crop, especially rice, to met the increasing demand of the rising population in 20243. It is importatnt to note that, the prediction was carried out without putting into consideration some factors such as economic, safety and security, ecological factors etc. Therefore, this prediction is liable to change, or might not occur exactly as shown.

5. Conclusion

The study reveals on reveals significant trends in urban growth and environmental dynamics in Argungu between 2009 and 2023, driven by factors such as population increase, economic activities, and improved infrastructure. Notably, built-up areas rose from 1.82% to 3.56%, indicating persistent urban sprawl characterized by low-density development radiating from the urban center (Argungu). The analysis utilized five (5) LULC classes namely; built-up areas, bare land, rock, water bodies, and vegetation, highlighting complex interactions influenced by climate events and human activities. Furthermore, the application of Shannon's entropy illustrated an increasing diversity in land use patterns, pointing to more scattered and varied urban growth, which may pose challenges for infrastructure and resource management. These findings emphasize the necessity for sustainable urban planning strategies in Argungu that reconcile development with environmental preservation to ensure a resilient and sustainable future for the region. Given the significant impact of flooding on land cover changes, it is essential to develop and implement effective flood management strategies. Government and other stakeholders should establish a framework for continuous monitoring of LULC changes using remote sensing and GIS technologies. This will enable timely assessments of urban growth patterns, environmental changes, and the effectiveness of implemented policies.

References

Ankrah, D., Takyi, S.A., Biliyitorb Liwur, S., Amponsah, O., 2024. Urban sprawl, urban form, and urban land use pattern: examining urban planning response to the causes and effects of urban sprawl in Kumasi, Ghana. *African Geographical Review*, 1–15. https://doi.org/10.1080/19376812.2024.2391777.

Behera, A., Rawat, K.S., Kumar, S., Almuflih, A.S., Almakayeel, N., Qureshi, M.R.N., 2025. Simulation and projection of land use and land cover using remote sensing data and CA–Markov model case study. *Geocarto International*, 40(1). https://doi.org/10.1080/10106049.2025.2450441.

Bielecka, E., 2020. GIS spatial analysis modeling for land use change. A bibliometric analysis of the intellectual base and trends. *Geosciences*, 10(11), 421. https://doi.org/10.3390/geosciences10110421.

Earth Resources Observation and Science (EROS) Center, 2020a. *Landsat 7 Enhanced Thematic Mapper Plus Level-2, Collection 2 [dataset].* U.S. Geological Survey. https://doi.org/10.5066/P9C7I13B.

Earth Resources Observation and Science (EROS) Center, 2020b. *Landsat 8-9 Operational Land Imager / Thermal Infrared Sensor Level-2, Collection 2 [dataset].* U.S. Geological Survey. https://doi.org/10.5066/P9OGBGM6.

Isma'il, M., Ishaku, E., Yahaya, A.M., Tanko, M.A., Ahmed, H.T., 2015. Urban growth and housing problems in Karu local government area of Nasarawa State, Nigeria. *Global J. Res. Rev*, 2, 45- 57. https://hal.science/hal-03714379.

Jaeger, J.A., Bertiller, R., Schwick, C., Kienast, F., 2010. Suitability criteria for measures of urban sprawl. *Ecological Indicators*, 10(2), 397-406. https://doi.org/10.1016/j.ecolind.2009.07.007.

Lawal, I.A., Gulma, U.L., 2024. Assessment of land use and land cover change detection for Argungu Urban: A Remote Sensing and GIS Approach. *International Journal of Science and Research Archive,* 13(02), 1434–1439. https://doi.org/10.30574/ijsra.2024.13.2.2278.

Musa, K., Abubakar, M.L., 2024. Monitoring urban growth and landscape fragmentation in Kaduna, Nigeria, using remote sensing approach. *Journal of Degraded & Mining Lands Management,* 12(1). https://doi.org/10.15243/jdmlm.2024.121.6757.

Nyamekye, C., Kwofie, S., Agyapong, E., Ofosu, S. A., Arthur, R., Appiah, L.B., 2021. Integrating support vector machine and cellular automata for modelling land cover change in the tropical rainforest under equatorial climate in Ghana. *Current Research in Environmental Sustainability*, 3, 100052. https://doi.org/10.1016/j.crsust.2021.100052.

Sadigov, R., 2022. Rapid Growth of the World Population and Its Socioeconomic Results. *The Scientific World Journal*, *2022*, 8110229. https://doi.org/10.1155/2022/8110229.

Sajan, B., Mishra, V.N., Kanga, S., Meraj, G., Singh, S.K., Kumar, P., 2022. Cellular Automata-Based Artificial Neural Network Model for Assessing Past, Present, and Future Land Use/Land Cover Dynamics. *Agronomy*, 12(11), 2772. https://doi.org/10.3390/agronomy12112772.

Sakizadeh, M., Milewski, A., 2024. Quantifying LULC changes in Urmia Lake Basin using machine learning techniques, intensity analysis and a combined method of cellular automata (CA) and artificial neural networks (ANN) (CA-ANN). *Model. Earth Syst. Environ.*, 10, 2011–2030. https://doi.org/10.1007/s40808-023-01895-z.

Shikary, C., Rudra, S., 2021. Measuring Urban Land Use Change and Sprawl Using Geospatial Techniques: A Study on Purulia Municipality, West Bengal, India. *Journal of the Indian Society of Remote Sensing*, 49(2), 433–448. https://doi.org/10.1007/s12524-020-01212-6.

Steurer, M., Bayr, C., 2020. Measuring urban sprawl using land use data. *Land Use Policy*, 97, 104799. https://doi.org/10.1016/j.landusepol.2020.104799.

Taloor, A.K., Kumar, V., Singh, V.K., Singh, A.K., Kale, R.V., Sharma, R., Khajuria V., Raina, G., Kouser, B., Chowdhary, N.H., 2020. Correction to: land use land cover dynamics using remote sensing and GIS techniques in Western Doon Valley, Uttarakhand, India. *Geoecology of Landscape Dynamics*. doi: 10.1007/978-981-15-2097-6_4.

Wiatkowska, B., Słodczyk, J., Stokowska, A., 2021. Spatial-temporal land use and land cover changes in urban areas using remote sensing images and GIS analysis: The case study of Opole, Poland. *Geosciences*, 11(8), 312. https://doi.org/10.1007/978-981-15-2097-6_23.

Zhu, Q., Zeng, M., Jia, P., Guo, M., Liang, X., Guan, Q., 2024. Measuring the urban sprawl based on economic-dominated perspective: the case of 31 municipalities and provincial capitals. *Geo-Spatial Information Science*, 27(4), 1272–1289. https://doi.org/10.1080/10095020.2023.2202201.